REFERENCES

1. I.J. Bahl and P. Bhartia, Microstrip antennas, Artech House, Dedham, MA, 1980.
2. J.R. James, P.S. Hall, and C. Wood, Microstrip antennas-theory and design, Peter Peregrinus Ltd., London, 1981.
3. K.C. Gupta and A. Benalla (Eds.), Microstrip antenna design, Artech House, Canton, MA, 1988.
4. J.R. James and P.S. Hall, Handbook of microstrip antennas, vols. 1 and 2, IEE Electromagnetic Wave Series 28, Peter Peregrinus Ltd., London, 1989.
5. Y.T. Lo, S.M. Wright, and M. Davidovitz, "Microstrip Antennas," K. Chang (Ed.), Handbook of microwave and optical components, vol. 1, Wiley, New York, 1989, pp. 764–889.
6. P. Bhartia, K.V.S. Rao, and R.S. Tomar (Eds.), Millimeter-wave microstrip and printed circuit antennas, Artech House, Canton, MA, 1991.
7. K. Hirasawa and M. Haneishi, Analysis, design, and measurement of small and low-profile antennas, Artech House, Canton, MA, 1992.
8. D.M. Pozar and D.H. Schaubert (Eds.), Microstrip antennas—the analysis and design of microstrip antennas and arrays, IEEE Press, New York, 1995.
9. J.F. Zurcher and F.E. Gardiol, Broadband patch antennas, Artech House, Norwood, MA, 1995.
10. R.A. Sainati, CAD of microstrip antennas for wireless applications, Artech House, Norwood, MA, 1996.
11. K.F. Lee and W. Chen, Advances in microstrip and printed antennas, Wiley, New York, 1997.
12. K.L. Wong, Design of nonplanar microstrip antennas and transmission lines, Wiley, New York, 1999.
13. R. Garg, P. Bhartia, I. Bahl, and A. Ittipiboon, Microstrip antenna design handbook, Artech House, Canton, MA, 2001.
14. K.L. Wong, Compact and broadband microstrip antennas, Wiley, New York, 2002.
15. T. Itoh and R. Mittra, Analysis of a microstrip disk resonator, AEU Int J Electron Commun 27 (1973), 456–458.
16. J.Q. Howell, Microstrip antennas, IEEE Trans Antennas Propagat AP-23 (1975), 90–93.
17. S.A. Long, L.C. Shen, M.D. Walton, and M.R. Allerding, Impedance of a circular disk printed-circuit antenna, Electron Lett 14 (1978), 684–686.
18. K.R. Carver, Practical analytical techniques for the microstrip antenna, Proc Wkshp Printed Circ Antenna Technol, Las Cruces, New Mexico, 1979, pp. 7.1–7.20.
19. W.C. Chew and J.A. Kong, Analysis of a circular microstrip disk antenna with a thick dielectric substrate, IEEE Trans Antennas Propagat AP-29 (1981), 68–76.
20. S. Yano and A. Ishimaru, A theoretical study of the input impedance of a circular microstrip disk antenna, IEEE Trans Antennas Propagat AP-29 (1981), 77–83.
21. J.S. Dahele and K.F. Lee, Effect of substrate thickness on the performance of a circular-disk microstrip antenna, IEEE Trans Antennas Propagat AP-31 (1983), 358–360.
22. J.S. Dahele and K.F. Lee, Theory and experiment on microstrip antenna with air gaps, IEE Proc Pt H 132 (1985), 455–460.
23. M. Davidovitz and Y.T. Lo, Input impedance of a probe-fed circular microstrip antenna with thick substrate, IEEE Trans Antennas Propagat AP-34 (1986), 905–911.
24. F. Abboud, J.P. Damiano, and A. Papiernik, New determination of resonant frequency of circular disc microstrip antenna: application to thick substrate, Electron Lett 24 (1988), 1104–1106.
25. K. Antoszkiewicz and L. Shafai, Impedance characteristics of circular microstrip patches, IEEE Trans Antennas Propagat AP-38 (1990), 942–946.
26. V. Losada, R.R. Boix, and M. Horno, Resonant modes of circular microstrip patches in multilayered substrates, IEEE Trans Microwave Theory Tech MTT-47 (1999), 488–497.
27. J.-S.R. Jang, ANFIS: adaptive-network-based fuzzy inference system, IEEE Trans Systems Man and Cybernetics 23 (1993), 665–685.
28. J.-S.R. Jang, C.T. Sun, and E. Mizutani, Neuro-fuzzy and soft computing: a computational approach to learning and machine intelligence, Prentice-Hall, Upper Saddle River, NJ, 1997.
29. Q.J. Zhang and K.C. Gupta, Neural networks for RF and microwave design, Artech House, Boston, MA, 2000.
30. C.G. Christodoulou and M. Georgiopoulos, Application of neural networks in electromagnetics, Artech House, MA, 2001.
31. E. Bokshtein, D. Shmaltz, O. Herbst, H. Bunke, and A. Kandel, Monopulse amplitude direction-finding using neuro-fuzzy approach, Robotics Autonomous Syst 33 (2000), 125–134.
32. K. Guney and N. Sarikaya, Computation of resonant frequency for equilateral triangular microstrip antennas with the use of adaptive neuro-fuzzy inference system, Int J RF and Microwave CAE 14 (2004), 134–143.
33. K. Guney and N. Sarikaya, Adaptive neuro-fuzzy inference system for the input resistance computation of rectangular microstrip antennas with thin and thick substrates, J Electromagn Waves Applic (JEWA) 18 (2004), 23–39.
34. K. Guney and N. Sarikaya, Adaptive neuro-fuzzy inference system for computing the resonant frequency of circular microstrip antennas, Applied Computat Electromagn Soc J 19 (2004), 188–197.
35. K. Guney and N. Sarikaya, Input resistance calculation for circular microstrip antennas using adaptive neuro-fuzzy inference system, Int J Infrared Millimeter Waves 25 (2004), 703–716.
36. K. Guney and N. Sarikaya, Adaptive neuro-fuzzy inference system for the computation of the bandwidth of electrically thin and thick rectangular microstrip antennas, Electrical Engineering (Archiv fur Elektrotechnik) 88 (2006), 201–210.
37. I. Turkmen and K. Guney, Cheap joint probabilistic data association with adaptive neuro-fuzzy inference system state filter for tracking multiple targets in cluttered environment, AEU-Int J Electron Commun 58 (2004), 349–357.
38. W.C. Chew and J.A. Kong, Effects of fringing fields on the capacitance of circular microstrip disk, IEEE Trans Microwave Theory Tech MTT-28 (1980), 98–104.

DISTURBANCE OF MEASUREMENT PROBE FOR EXPOSURE ASSESSMENT OF A BASE STATION ANTENNA NEAR A GROUND PLANE

Wout Joseph, Laurens Roelens, and Luc Martens
Department of Information Technology
Ghent University
Interdisciplinary Institute for BroadBand Technology (IBBT)
Gaston Crommenlaan 8 box 201
B-9050 Ghent, Belgium

Received 7 February 2006

ABSTRACT: *The disturbance caused by a measurement probe close to a ground plane is characterized. A trade-off must be made between disturbance and sensitivity. An optimal probe for electromagnetic exposure measurements above a ground plane in the neighborhood of a base station antenna is selected.* © 2006 Wiley Periodicals, Inc. Microwave Opt Technol Lett 48: 1610–1613, 2006; Published online in Wiley InterScience (www.interscience.wiley.com). DOI 10.1002/mop.21694

Key words: *disturbance; base station antenna; electromagnetic radiation; measurement probe*

1. INTRODUCTION

For exposure assessment around a base station antenna, the electromagnetic fields must be determined and be compared to the reference levels [1]. Being able to perform accurate electromagnetic field measurements "in the field" is thus important. The measurement of electromagnetic fields will be disturbed by the measurement probes themselves and by the presence of material interfaces such as the ground plane. To obtain an accurate estimation of human exposure, the electromagnetic fields have to be averaged over the volume of the body of a person [1, 2]. However, obtaining the average would require many measurements over a the volume of a person and would be too time-consuming. Therefore measurements are mostly performed at a single point resulting in a less accurate estimate of the actual exposure [3]. Knowledge of the field at different locations in a plane or over a vertical line, representing the length of an average human, results in a better estimate of the exposure [2]. However, close to the ground plane, the measurement probe will be disturbed. This disturbance cannot be fully taken into account by the calibration. The objective of this paper is to show that when the disturbance must be limited to a predefined value (e.g., 5%), a suitable measurement probe with maximal sensitivity can be selected even when performing measurements close to the ground. Investigation of the disturbance of the measurement probe near an interface is evaluated by means of a numerical field computation method. The method of moments (NEC-code) is a suitable tool for that purpose.

2. METHOD

2.1. Configuration

We will simulate an exposure "measurement" in the neighborhood of a K736863 GSM base station using simulations with NEC-Win-Pro®. The K736863 antenna radiates at 900 MHz and is positioned 30 m above a ground plane (average ground, conductivity $\sigma = 0.005$ S/m and permittivity $\varepsilon_r = 13$). The simulated "measurements" will be performed as a function of the height from 1 cm to 1.75 m (corresponding with the length of an average man [5]) above the ground at 200 m from the base station antenna. This configuration represents a realistic exposure situation for the general public [3, 4]. The "measurement" configuration and coordinate system are shown in Figure 1 (not to scale). A typical input power of 20 W for the base station antenna is used [6]. In this paper, only the electric field is investigated because a GSM base station antenna is an electrical source resulting in a dominant E-field [3, 4, 6] (see section 3.1.). Analysis of the magnetic field can be performed analogously.

2.2. Procedure

We now will describe the subsequent steps of the procedure to study the disturbance of a field probe near an interface.

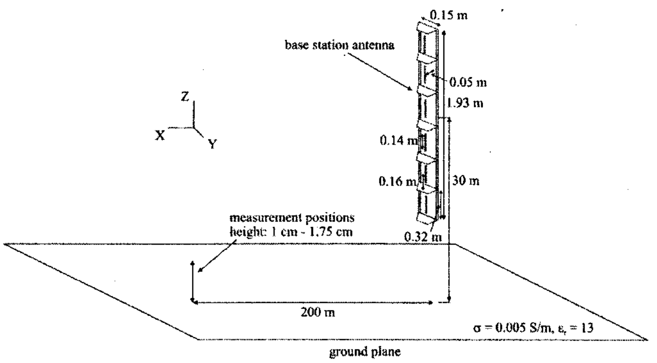

Figure 1 Configuration of the exposure "measurement" in the neighborhood of a base station antenna with an input power of 20 W as a function of the height above the ground plane

2.2.1. Simulation of the True Field

In this step, the true field of the transmitting antenna Tx, noted as E^{true} will be simulated. The extended thin-wire kernel of the NEC-program is used because in some of the simulations, the ratio of segment length to wire radius is small. An applied E-field source model (that is, an applied voltage over the source segment) is used and the length of the source segment is made equal to the length of the other segments.

2.2.2. Calibration

The simulated calibration is a two-antenna method. In the first step, the free-space far field E^i of a calibration antenna is simulated. In the second step, the configuration with the calibration antenna and the measurement probe located in the far field, is simulated. The measurement probe is terminated with a 50Ω resistance (in practice, measurements are performed with a 50Ω measurement system, e.g., a spectrum analyzer) and the "measured" voltage V is determined.

Finally, the antenna factor (AF) is derived using formula (1):

$$\text{AF} = 20 \cdot \log\left(\frac{E^i}{V}\right) [\text{dB (1/m)}] \tag{1}$$

where E^i is the electric field incident on the antenna to be calibrated and V is the voltage developed across the output of the antenna to be calibrated.

2.2.3. Measurement of the Field

Once the measurement probe or receiving antenna Rx is calibrated, the field of Tx can be measured by determining the voltage V across the 50Ω output of the antenna. Using the antenna factor of formula (1), three orthogonal magnitudes of the field are "measured". From these three magnitudes E_k, ($k = 1, 2, 3$) the total field $E_{\text{tot}}^{\text{meas}} = \sqrt{E_1^2 + E_2^2 + E_3^2}$ is obtained. This total field will then be compared to the reference levels for the general public at 900 MHz [1].

The measurement probes under study are dipoles noted as Dy (Dy stands for dipole with length y times the wavelength at 900 MHz). The dipoles have a length of 1 cm (D0.03λ), 3 cm (D0.10λ), 7.5 cm (D0.23λ, about λ/4), 11.3 cm (D0.34λ), and 15 cm (D0.45λ, about λ/2), respectively. The radius of the wire of the dipoles is 1.8 mm.

2.2.4. Comparison of the True and Measured Values

The relative deviation $\mathfrak{F}$ [%] of fields measured by the probe with respect to the true field is determined as follows:

$$\mathfrak{F} = \left[\frac{E^{\text{true}} - E_{\text{tot}}^{\text{meas}}}{E^{\text{true}}}\right] \cdot 100 \tag{2}$$

The relative deviation $\mathfrak{F}$ will be called the disturbance of the measurement probe. Finally, an optimal measurement probe with maximal sensitivity (low AF) and with a disturbance smaller than, e.g., 5% can be selected.

3. RESULTS

3.1. True Field

First, the ratio of the true electric (E^{true}) and true magnetic (H^{true}) field of the K736863 base station antenna is analyzed. Figure 2 shows $Z^{\text{true}} = E^{\text{true}}/H^{\text{true}}$ as a function of the height above the ground plane at 200 m from the base station antenna. Z^{true} is higher than the free-space value of 377Ω with a maximal value of 580Ω

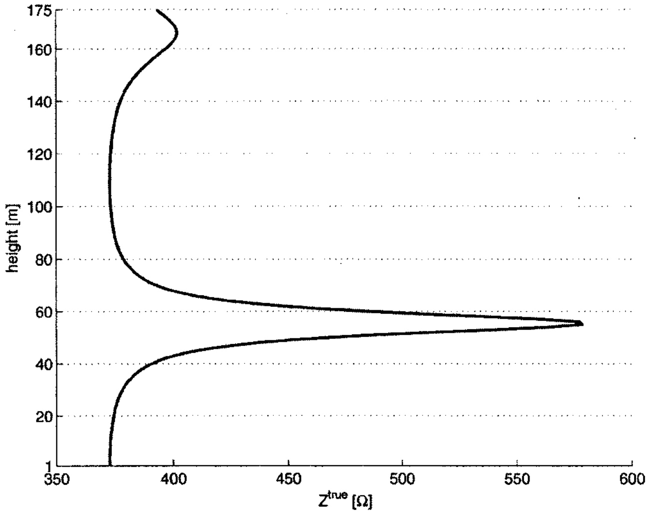

Figure 2 The ratio Z^{true} of the true electric and true magnetic field as a function of the height above the ground plane

at about 60 cm (see section 3.3). This shows that the E-field is dominant, resulting in the worst case for electromagnetic exposure [3, 4, 6]. Therefore we analyze in this paper only the electric field (as mentioned in section 2.1.).

Figure 3 shows the true electric field E^{true} at x = 199, 200, and 201 m as a function of the height above the ground plane. These values do not differ much due to the far-field condition of the investigated configuration (200 m > far-field distance of 22.3 m for K736863 antenna at 900 MHz) and the small angle of incidence (only 8.6°, Fig. 1) [4]. The relative deviation of the field values at 200 m and the values at 200 m ± 1 m is maximally 3.9%. This maximal deviation decreases to 0.6% for values at 200 m and 200 m ± 0.14 m (width of average man is about 0.28 m [5]). Thus, the variation over distances representing the volume of a human body in the x-direction (and analogously for the y-direction) is small compared to the variation as a function of the height above the ground plane (z-direction). Therefore, the analysis of the field at locations over a vertical line results in a better estimate of the exposure compared to the analysis at a single point [2]. In the following of this paper, we will thus analyze the electric field at 200 m.

TABLE 1 Antenna Factor, Threshold Value, and Ranges of Different *Rx* for Simulated "Measurements" by a Spectrum Analyzer for the Investigated Configuration at 900 MHz

Length Rx/λ	AF [dB (1/m)]	E_{th} [mV/m]	Range $E > E_{th}$ [cm]
0.03	71.3	823	N
0.1	57.3	163	1–28.3/85.6–142.5
0.23	44.0	34.5	1–175
0.34	33.7	10.8	1–175
0.45	27.3	5.2	1–175

N = Not in the considered range of heights

3.2. Determination of Threshold Value

To obtain frequency-dependent measurements, a spectrum analyzer (SA) is used [2, 3]. The noise floor, for example, of the HP8561B spectrum analyzer, is −70 dBm for a resolution bandwidth of 300 kHz (the resolution filter of 300 kHz is the smallest filter of the HP8561B spectrum analyzer that can contain the entire 200-kHz GSM frequency channel). Taking a required signal-to-noise ratio of 10 dB into account and using the AF of the different Rx, results in a treshold value for the electric field for the different Rx. Table 1 shows the antenna factor at 900 MHz and the treshold value E_{th} [V/m] for the different Rx. The smaller the Rx, the less sensitive the Rx (high value for AF) and the higher the treshold value: for example, D0.45λ is about 30 times more sensitive than D0.1λ (Table 1).

3.3. Selection of Optimal Rx

Figure 4 shows the true electric field E^{true} and the corresponding treshold values E_{th} for the different Rx at 200 m from the base station antenna. This figure shows that D0.03λ is not sufficiently sensitive to perform the measurements of this configuration with a SA ($E_{th}^{D0.03\lambda} > E^{true}$). D0.1λ is only sensitive enough for some specific ranges (see also Table 1). The other dipoles are sufficiently sensitive to perform the measurements above the ground plane. This figure also shows that the field values are below the reference levels for exposure of the general public: the maximum (0.23 V/m)

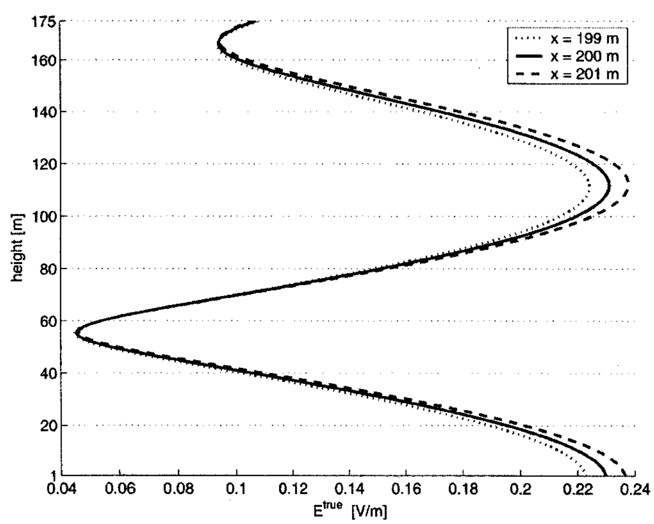

Figure 3 The true electric field of the 900 MHz-base station antenna with an input power of 20 W at x = 199, 200, and 201 m as a function of the height above the ground plane

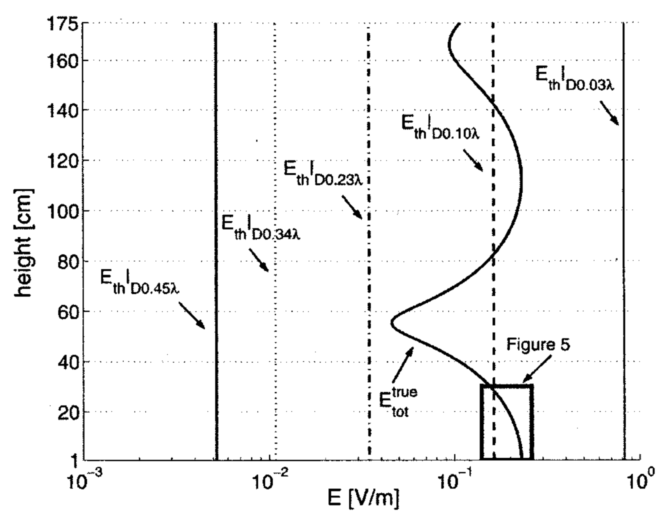

Figure 4 The true electric field at 200 m of the 900 MHz-base station antenna with an input power of 20 W as a function of the height above the ground plane and the treshold value for the different Rx

and average (0.16 V/m) electric field in the considered range of heights are about 180 and 260 times below the ICNIRP reference level of 41.3 V/m at 900 MHz [1], respectively.

Figure 5 zooms in on Figure 4 and compares E^{true} with the measured field values from 1 to 30 cm above the ground. Only the smallest dipoles are capable to perform accurate measurements: D0.1λ enables measurements close to the ground plane with sufficient accuracy ($\mathfrak{F} < 5\%$). D0.03λ would even perform better but is not shown in Fig. 5 since this dipole is not sufficiently sensitive.

Figure 6 shows the disturbance $\mathfrak{F}$ for different Rx as a function of the height above the ground. Also the lines for $\mathfrak{F}$ equal to 1%, 5%, and 10% are shown. This figure shows that lower deviations occur when a smaller Rx is used. The disturbance is maximal close to the ground plane and has a local maximum at about 60 cm due to the fact that the x-component of the electric field—which is parallel with the ground plane and thus suffers the highest coupling with the ground plane—reaches a local maximum at about 60 cm and is then dominant (otherwise the z-component is dominant, Fig. 1). At this height, Z^{true} reaches a maximum, as shown in Figure 2. This can be explained by the fact that the components of the magnetic field do not reach a maximum in contrary to the x-component of the electric field. Therefore the electric field is relatively stronger at this height compared to the magnetic field, resulting in a maximal value for $Z^{\text{true}} = E^{\text{true}}/H^{\text{true}}$. The results presented in Figures 4, 5, and 6 show that a trade-off has to be made between sensitivity and disturbance (e.g., $\mathfrak{F} < 5\%$). Based on these results, we propose suitable probes for this configuration. For heights up to 28 cm, D0.1λ is a suitable measurement probe if $\mathfrak{F} < 5\%$ is required because D0.1λ is sufficiently sensitive up to 28 cm and has the smallest disturbance (Fig. 4 and Table 1). Above 28 cm, D0.23λ, which is more sensitive than D0.1λ, is the optimal measurement probe when disturbances lower than 5% are required. For heights larger than 62 cm and $\mathfrak{F} < 5\%$, D0.45λ—which is the most sensitive Rx (Table 1)—is the optimal measurement probe. If only $\mathfrak{F} < 10\%$ is required, then D0.45λ can be used from 10.4 cm above the ground plane for this configuration.

Using this procedure, an optimal probe, which is sufficiently sensitive and has a disturbance lower than a predefined value, can be selected for measurements near a ground plane.

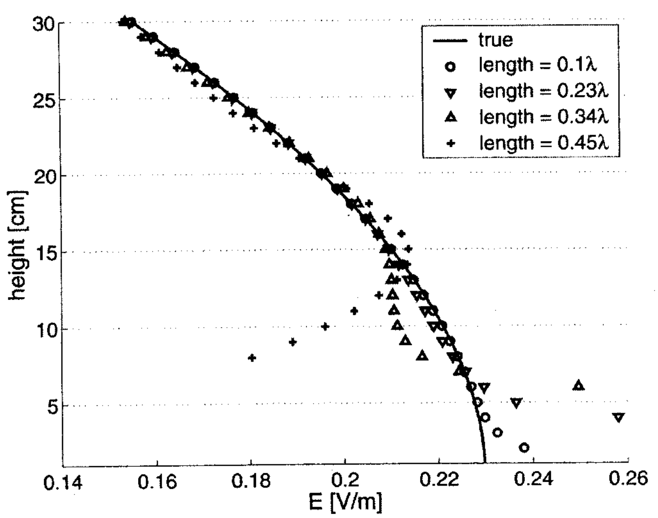

Figure 5 Zoom-in on Fig. 4 from 1 to 30 cm above the ground plane (— true, ○ length = 0.1λ, ▽ length = 0.23λ, △ length = 0.34λ, + length = 0.45λ)

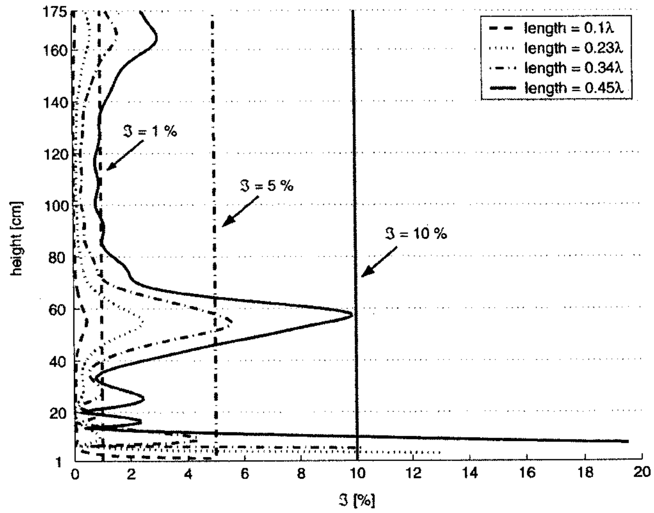

Figure 6 Disturbance $\mathfrak{F}$ for the different probes as a function of the height above the ground plane (– – – length = 0.1λ, · · · · · · · · · length = 0.23λ, – · – · length = 0.34λ, — length = 0.45λ)

4. CONCLUSION

For an electromagnetic exposure measurement above a ground plane and in the neighborhood of a base station antenna, an optimal measurement probe can be selected. A trade-off between disturbance and sensitivity of the measurement probe has to be made. Close to the ground plane, one has to select a small measurement probe with sufficient sensitivity to obtain a low disturbance (e.g., smaller than 5%). Higher above the ground plane, one can select larger and thus more sensitive measurement probes.

REFERENCES

1. International Commission on Non-ionizing Radiation Protection, Guidelines for limiting exposure to time-varying electric, magnetic, and electromagnetic fields (up to 300 GHz), Health Physics 74 (1998), 494–522.
2. CENELEC EN50383, Basic standard for the calculation and measurement of electromagnetic field strength and SAR related to human exposure from radio base stations and fixed terminal stations for wireless telecommunication systems (110 MHz to 40 GHz), 2002.
3. G. Neubauer, H. Haider, and K. Lamedschwander, Measurement methods and legal requirements for exposure assessment next to GSM base stations, Proc 15th Int Zurich Symp Electromagn Compat (2003), 143–148.
4. W. Joseph, L. Verloock, and L. Martens, Reconstruction of the polarization ellipse of the EM field of base station antennas by a fast and low-cost measurement method, IEEE Trans Electromagn Compat (2006), accepted.
5. H.M.C.H. Durney and M.F. Iksander, Radiofrequency Radiation Dosimetry Handbook (Fourth Edition), USAF School of Aerospace Medicine, Brooks Air Force Base (1997), http://www.brooks.af.mil/AFRL/HED/hedr/reports/handbook/contents.
6. W. Joseph and L. Martens, Comparison of safety distances of electromagnetic field and SAR for occupational exposure of a base station antenna, IEEE Trans Electromagn Compat EMC-54 (2005), 977–985.